Available online at www.sciencedirect.com

ScienceDirect

Procedia Structural Integrity 24 (2019) 178–189

Structural Integrity Procedia

www.elsevier.com/locate/procedia

AIAS 2019 International Conference on Stress Analysis

Proposal of a novel approach for 3D tooth contact analysis and calculation of the static transmission error in loaded gears

Fabio Bruzzone[a,b], Tommaso Maggi[a,b], Claudio Marcellini[a,b], Carlo Rosso[a,b*], Cristiana Delprete[a]

[a] *Politecnico di Torino, Corso Duca degli Abruzzi 24, Torino 10129, Italy*
[b] *GeDy TrAss, s.r.l., Gear Dynamic Transmission Analysis Company, Via Alfonso La Marmora 16, Torino 10128, Italy*

Abstract

The static transmission error in gears represents the main noise and vibration source of mechanical transmissions, both for self-excitation and for the excitation of powertrain components. An accurate determination of it is very complex, since it requires experimental tests or highly detailed models. In both cases the costs and the computational time are high, therefore the possible different types of geometries to analyse are significantly reduced. In the present work, a semi-analytical methodology is proposed, with the aim of evaluating the variation of the contact area in gears during their meshing and at different levels of applied torque. This model considers the tooth compliance (tooth shear and bending, foundation and rim, gear body) and the local contact effects. The present semi-analytical methodology allows a detailed analysis of the tooth compliance and the contact area on a high number of points along the meshing cycle (typically over 100 points). It also enables the definition of the correct contact area geometry between meshing teeth, depending on the possible geometry modification (micro-geometry and/or manufacturing errors) and on the input torque. In particular, the contact is simulated through a non-Hertzian model able to evaluate every contact shape, overcoming the limits of the Hertzian theory. The goal of the proposed methodology is to determine with high precision the static transmission error between gears in a limited time with respect to the classical finite element method. Furthermore, it is useful for a reliable prediction of the transmission dynamic behaviour, considering the load exchanged between the teeth in relation to spin speed and torque, in a computational time lower than the classical techniques.

Keywords: Gears; transmission error; tooth modifications; tip relief; crowning; Hertz; contact model

* Corresponding author. Tel.: +39-011-0905817; fax: +39-011-0906999.
E-mail address: carlo.rosso@polito.it

10.1016/j.prostr.2020.02.015

1. Introduction

The static transmission error (STE), which is the linear or angular difference between the ideal and theoretical position of the two engaging gears and the real and actual position of the same gears in operating conditions under load, is a fundamental parameter for the evaluation of the dynamic transmission error (DTE) in every gearbox application, that could lead to early failure of the mechanical components and to noise, vibration and harshness (NVH) phenomena. The peak-to-peak transmission error (PPTE), which is the difference of the STE when the lowest number of teeth couples is in contact and when the highest number of teeth couples is in contact for a specific contact ratio, is strictly influenced by the tooth profile modifications. In fact, they are obtained by cutting techniques useful to control and minimize the noise and vibration levels, in their turn related to the value of the PPTE under load. Furthermore, tip relief and crowning modifications of the teeth flank surfaces are fundamental when high power must be transmitted to the user.

As a matter of fact, standard geometries often lead to sudden overloads both when teeth approach and leave contact. Gears with no crowning or tip relief, or with undesired misalignment, experience edge contacts and their subsequent pressure peaks. Typical tip or root relief are obtained by cutting material with linear or parabolic trend, altering the surface continuity of the geometries. Whereas, crowning modifications consists of removing material along the face-width, with the aim of concentrating the load at the center of the tooth. Both techniques are necessary when the designer wants to control the load pattern of the gears and the contact areas. Many researches on contact analysis starting from Johnson (1985) have been conducted. He developed different numerical methods to solve the limitation imposed by non-Hertzian problems. Indeed, he affirmed that “many non-Hertzian contact problems do not permit analytical solutions in closed form”. Beghini and Santus (2004) managed to settle the limitation of the Hertzian theory related to the symmetry of the profiles near the contact using an analytical cubic formulation for the description of non-standard shapes. Different approaches were conducted by Li and Berger (2003) and by Boedo (2013) that developed some semi-analytical models to solve general non-Hertzian normal contact mechanical problems. With similar methodologies, Marmo et al. (2016, 2018) developed a numerical-analytical procedure for the evaluation of contact problems for non-conforming bodies. The authors, starting with a 2D contact model for spur gears, validated with other commercial software described in Rosso et al. (2019), have improved the complexity of the model to analyze every type of gear with generic tooth and gear body shapes.

Having an accurate simulation software is mandatory because experimental analyses for the measurement of the real STE are extremely expensive, both for the high precision and accuracy of the sensors and for the flexibility of the test setup for different types of configurations, for instance spur, helical, bevel, spiral-bevel and planetary gears. Therefore, in this paper a flexible and fast Semi-Analytical (SA) methodology for the computation of the STE is presented. The code can compute all types of gears’ deflections, for instance tooth shear and bending, root and rim, gear body and local contact deformations. From them it afterwards derives the STE, receiving few input data such as the load condition, the material properties and the tooth and gear body geometries. Previous analysis had evaluated the main difference between beam and solid finite elements under static load. During this test, it was demonstrated that the beam element is not affected by the local effect, in contrast to the solid one in which it is the main source of displacement. For this reason, in the present work a focus on the evaluation of the local pressure distribution, peak pressure at the edges and gear contact areas and deformation is done, since the local contact is the most sensitive phenomenon to geometric variation of the components. Different cases of spur and helical gears with tooth surface modifications are presented and the principal discrepancies between these cases are highlighted. Finally, conclusion and future developments are discussed.

2. Three-dimensional non-Hertzian contact model

Referring to Figure 1, in the present work the STE is considered as the angular displacement measured in radiant when an input torque makes the pinion rotate with $\dot{\theta} \approx 0$ rad/s. The algorithm of the SA methodology is reported in Rosso et al. (2018) and resumed in Figure 2.

For the STE evaluation, the quasi-static and SA model is presented. Firstly, the algorithm calculates the pressure distribution exchanged between the two surfaces in contact and the total amount of the transferred force; afterwards, it detects all the deformations occurring within the meshing. In particular, the local deformation through the SA

method. The tooth shear and bending, root and rim, gear body displacements are calculated analytically. After that, the condition of the deformed gears under load is translated into the evaluation of the STE, considered as the delay of the working gears with respect to the theoretical and infinitely rigid bodies. Once this calculation is completed, the code turns the gears to the next angular position until a defined number of pitch angles is reached.

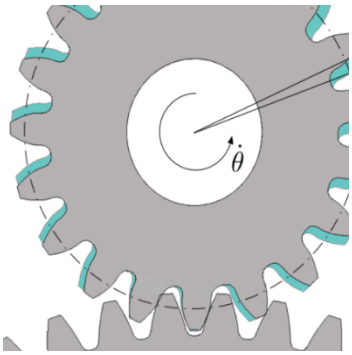

Fig. 1. Static transmission error (STE); in cyan the ideal position of the driver.

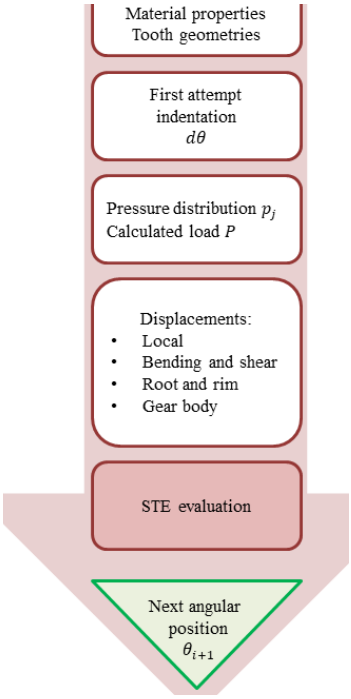

Fig. 2. Semi-analytical (SA) model for the STE evaluation.

2.1. Input parameters

The SA model requires three main categories of input parameters. For the material of the components, the user should insert the Young modulus, Poisson coefficient and density; the load condition is represented by the nominal torque of the operating condition and this value is set as the convergence criterion of the iterative calculation.
Furthermore, with few fundamental parameters of the gears, the code obtains the Cartesian coordinates of the points that describe the involute profiles with any type of modification. Therefore, the input parameters required for the geometric coordinates are listed in Table 1, distinguishing the pinion (Gear1) from the driven gear (Gear2) and their parameters with subscript 1 and 2. It would be possible to insert also other parameters such as the backlash, addendum and dedendum coefficients, that are here taken as standard values. With these values the code calculates automatically the three-dimensional coordinates of the cloud points that describe the gears. However, it is possible to insert already existing geometries with the appropriate characteristics. Spur and helical gears with tip relief or crowning are here considered.

Table 1. Input parameters for the geometric coordinates of the gears.

Gear parameters	Gear1 nomenclature	Gear2 nomenclature
Number of teeth [-]	z_1	z_2
Tooth module [mm]	m	m
Face-width [mm]	b_1	b_2
Pressure angle [°]	θ	θ
Helix angle [°]	β	β
Hub radius [mm]	r_{hub1}	r_{hub2}
Tip relief amount of modification [mm]	ΔC_{a1}	ΔC_{a2}
Tip relief height [mm]	ΔL_{a1}	ΔL_{a2}
Crowning amount [mm]	ΔL_{c1}	ΔL_{c2}

Table 2. Input parameters for the materials of the gears and the load operating conditions.

Material and load	Gear1 nomenclature	Gear2 nomenclature
Young modulus [MPa]	E_1	E_2
Poisson coefficient [-]	ν_1	ν_2
Density [$\mathrm{ton/m^3}$]	ρ_1	ρ_2
Input torque [Nmm]	C_1	

Table 3. Input parameters for the geometric coordinates of the gears in Cases 1, 2a, 2b and 3.

Gear parameters	Gear1 nomenclature	Gear2 nomenclature
Number of teeth [-]	30	30
Tooth module [mm]	3	3
Face-width [mm]	20	20
Hub radius [mm]	35	35
Pressure angle [°]	20	20
Helix angle (Case 3) [°]	30	30
Tip relief amount of modification (Case 3) [mm]	0.05	0.05
Tip relief height (Case 3) [mm]	1	1
Crowning amount (Case 2a) [mm]	0.008	0.008
Crowning amount (Case 2b) [mm]	0.5	0.5

With regards to the material and the load conditions, the input parameters are listed in Table 2. The test cases analyzed in the present work are listed in Table 3.

2.2. Non-Hertzian contact model

To compute the forces exchanged between the engaged teeth and the resultant local displacements, the pressure distribution must be calculated. The algorithm already developed by the authors (see Figure 3) has been extended to the 3D case to analyze all the non-conforming contact conditions between generic types of geometries. As teeth are getting in contact, a first attempt local displacement h_i, in the contact direction, is calculated as the superposition respectively of the surface of pinion's teeth and driven gear's teeth for each of the $i = 1, \dots, N$ points inside each contact area. After that, from the h_i value it is possible to obtain the pressure distribution p_i of each node and the total exchanged load P divided among the meshing couples of teeth j (P_j).
This procedure is repeated iteratively adjusting the indentation until the difference between P^*, obtained from the input torque, and P is lower than an imposed tolerance. The convergence criterion of the algorithm is that the total amount of load and transmitted torque is maintained. The model has been already validated with classical test cases, however an ulterior validation is here shown.

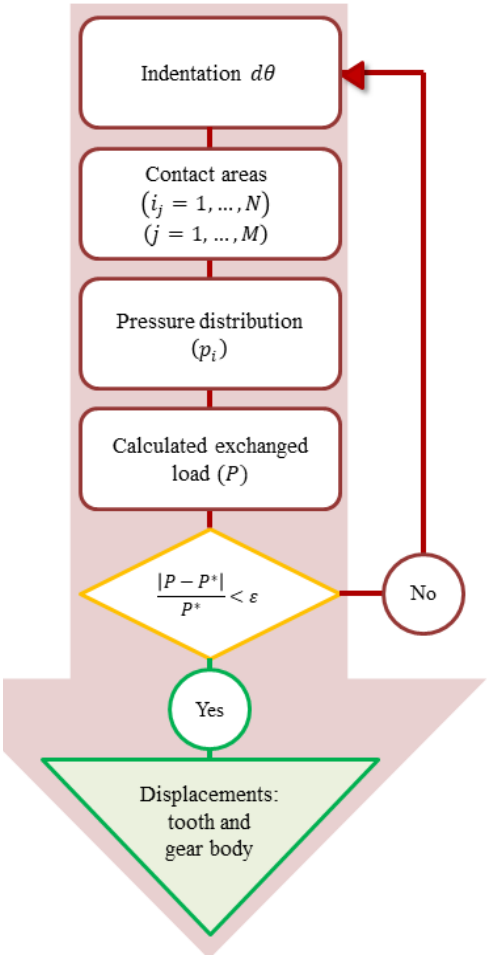

Fig. 3. Non-Hertzian contact algorithm.

2.3. Pressure distribution, contact area and pressure peaks

The cases presented in Table 3 are considered for the analysis of the pressure distribution, contact area and pressure peaks. Furthermore, to appreciate the variation of the contact area the analysis is conducted by applying increasing torque 100, 300 and 500 Nm, and considering two levels of crowning: $\Delta L_{c1,1} = \Delta L_{c2,1} = 0.008$ mm (Case 2a) and $\Delta L_{c1,2} = \Delta L_{c2,2} = 0.5$ mm (Case 2b).

In Figures from 4 to 8 the pressure distributions on the tangential contact plane between the meshing teeth are shown; they are referred to the maximum value of pressure in a certain angular position among all the teeth engaged: blue color corresponds to a null value, red color to the highest pressure value.

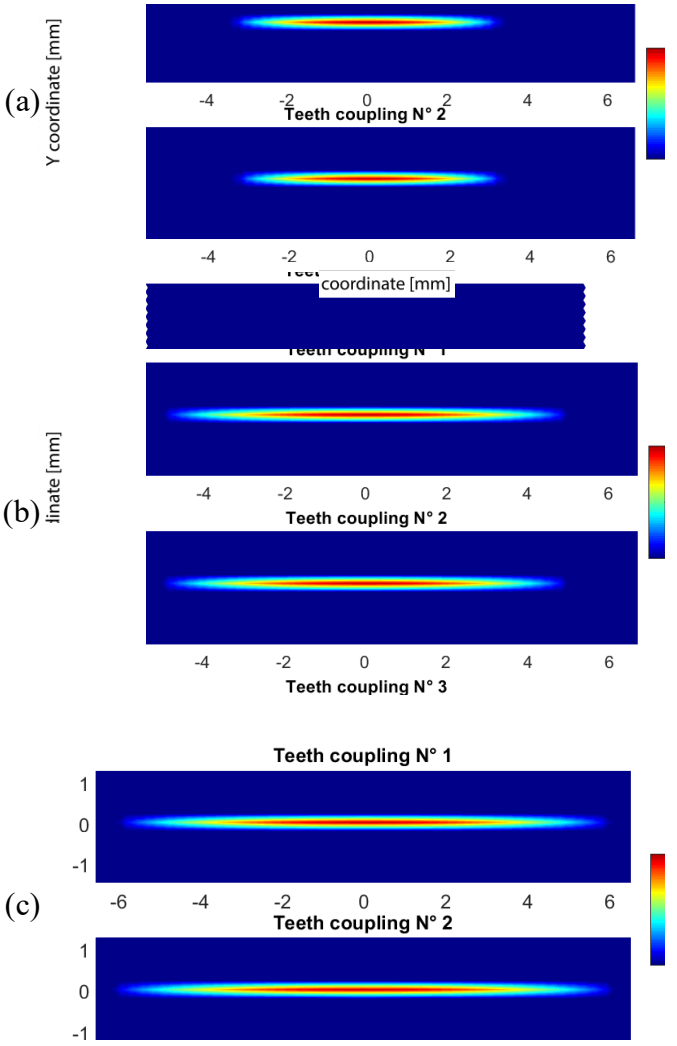

Fig. 4. Contact area variation for spur crowned gears (case 2a): (a) 100 Nm $p_{max} = 350$ MPa, (b) 300 Nm $p_{max} = 500$ MPa, (c) 500Nm $p_{max} = 700$ MPa.

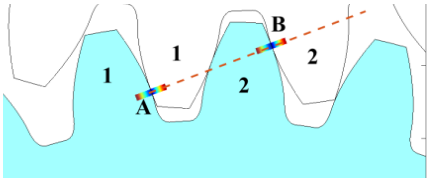

Fig. 5.1. Analyzed angular position; teeth couplings 1 and 2 and their rigid contact point A and B the along contact.

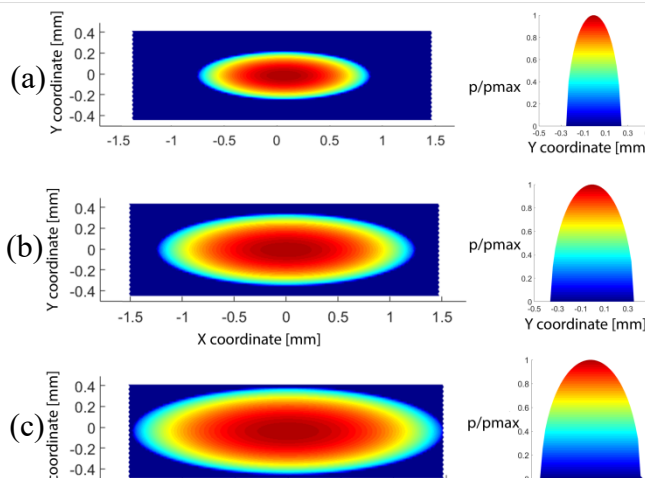

Fig. 5.2. Contact area variation for spur crowned gears (case 2b): (a) 100 Nm $p_{max} = 680$ MPa, (b) 300 Nm $p_{max} = 890$ MPa, (c) 500 Nm $p_{max} = 1050$ MPa.

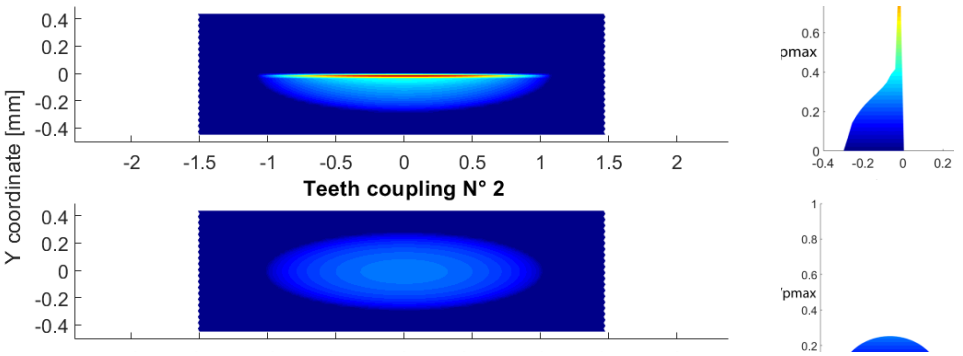

Fig. 6. Pressure distribution and peak before recessing of coupling 1 with 300 Nm and no tip relief (case 2b); $p_{max} = 850$ MPa.

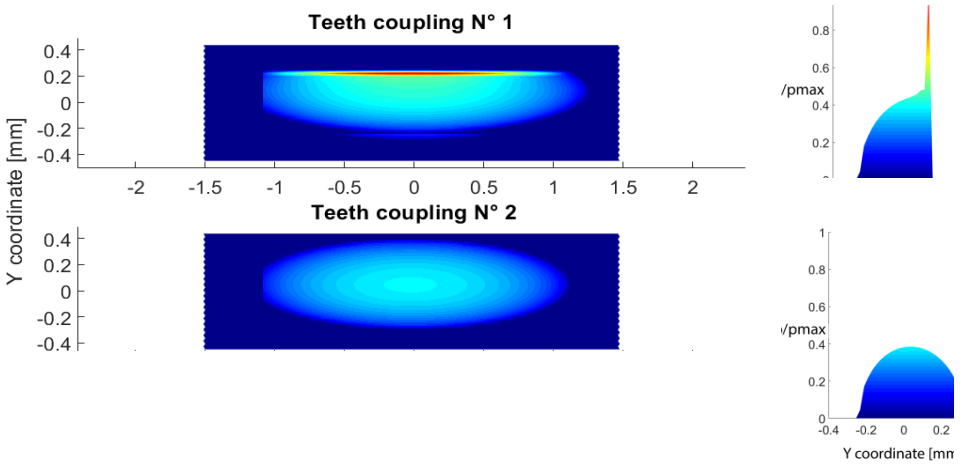

Fig. 7. Pressure distribution and peak with 300 Nm and linear tip relief (case 2b); $p_{max} = 630$ MPa.

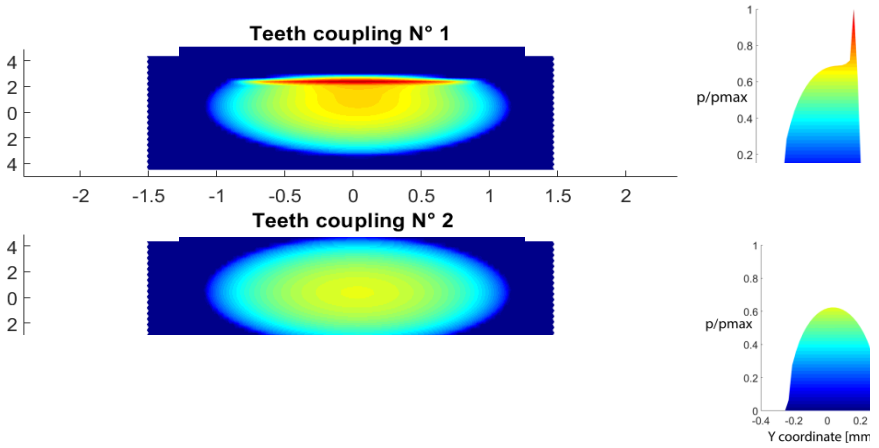

Fig. 8. Pressure distribution and peak with 300 Nm and parabolic tip relief (case 2b); $p_{max} = 575$ MPa.

Referring to Figure 4, it is clear that the contact area is larger at higher input torque: the width in X direction is about 6.5 mm at 100 Nm, 9.5 mm at 300 Nm and 12 mm at 500 Nm. Figure 5.1 shows the angular position analyzed both for Figure 4 and Figure 5.2: contact point A is in the first initial rigid contact, whereas contact B is entering the last section of the contact line. In Figure 5.2, the gears with $\Delta L_{c1,2}$ have been analyzed in a single-contact position near the pitch radius; this variation is useful to notice the influence of the incrementing torque on the variation of the contact area height. As a matter of fact, this effect is more noticeable when the value of tooth crowning is relatively high for this tooth geometry: $\Delta L_{c1,2} = 0.5$ mm makes the two curvatures in X and Y directions comparable. In the right side of the Figure 5.2 the p/p_{max} distribution along Y axis is shown. In figure 4 the torque increasing leads to an enlargement of the contact area with preferential X direction where the curvature is near 0 mm, whereas in Figure 5.2 the enlargements in both X and Y directions are comparable.

Figure 6 shows an angular position of the gears in Figure 5.2b), in which the teeth coupling 1 is about to leave the contact: it is noticeable that due to the absence of a tip relief modification, the tooth next to the recess condition has a peak of pressure all along the face-width at the tip, whereas the other coupling has a uniform distribution.

The influence of the tip relief modification on the same crowned spur gears is analyzed in Figures 7 and 8, with the same input torque 300 Nm. In the first case, there is a linear tip, whereas in the second case a parabolic tip relief with the same amount of material removal $\Delta C_a = 0.1$ mm and $\Delta L_a = 0.5$ mm. The comparison between the standard crowned gears and the ones with tip relief shows that the teeth with tip relief recess before the teeth without tip relief: respectively after 4.1053° and 5.4737° from their initial condition. Furthermore, the pressure distribution is better spread on a larger area in the teeth with tip relief leaving contact with respect to the same condition in standard crowned gears. The tip relief also allows a better distribution among the simultaneous contacting couples: in fact, the pressure peaks are lower than the standard case and the contact area in teeth coupling 2 has values closer to the maximum. In addition, the pressure distribution in parabolic tip relief case is more uniform than in the linear one, since the surface modification guarantees a lower discontinuity of material.

Figure 9 shows the pressure distributions for the spur crowned gear (Case 2a) at different values of the input torque.

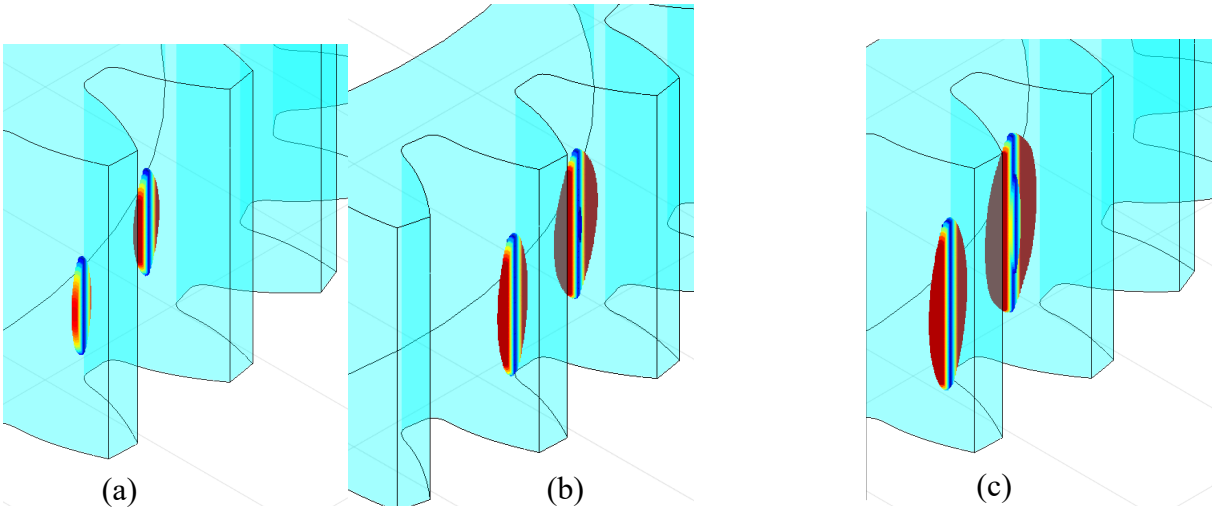

Fig. 9. Spur crowned gear (case 2a) pressure distribution and peaks: (a) 100 Nm $p_{max} = 680$ MPa, (b) 300 Nm $p_{max} = 890$ MPa, (c) 500 Nm $p_{max} = 1050$ MPa.

3. Semi-analytical model for displacements and STE evaluation

The non-Hertzian contact model explained in Section 2. provides the pressure distribution, pressure peaks and forces exchanged between two generic surfaces in contact. The force resultant inside the contact area is calculated and used as input of the SA model for the evaluation of tooth and gear body deformation and finally the STE. This model is based on an iterative determination of the contact point: due to the deformation of the tooth the position of the load application changes and the tooth's stiffness too.

3.1. Displacements

The displacements calculated through that methodology, are bending and shear deflection, root and rim displacement, local deformation and body displacement. In particular, the local deformation is the most significant in terms of magnitude. It is calculated using the non-Hertzian contact model and with the aim of validating the contact displacement a comparison with equivalent cases implemented in Finite Element (FE) model is shown. The shear and bending deflections are calculated using the formula proposed in Cornell (1981), the root and rim displacements are evaluated using the formula of Sainsot et al. (2004), and the gear body deformation is calculated using the formula of Attia (1964).

Three cases are compared with FE method:

- Case 1: standard spur gears;
- Case 2: spur gears with crowning;
- Case 3: helical gears and tip relief.

For simplicity, a singular angular position with a double contact for Case 1 and Case 2 comparisons is considered, whereas, due to the helix angle the contact becomes singular in Case 3. Therefore, two teeth have been analyzed for each gear both in the SA model and in the equivalent FE models. All the models are constrained in every degree of freedom at the bottom of the rim (red points in Figures 10 and 11). The static problems were solved by applying an input torque of 100 Nm, that generates a force distribution along the two teeth meshing flank represented by blue arrows in Figures 10 and 11.

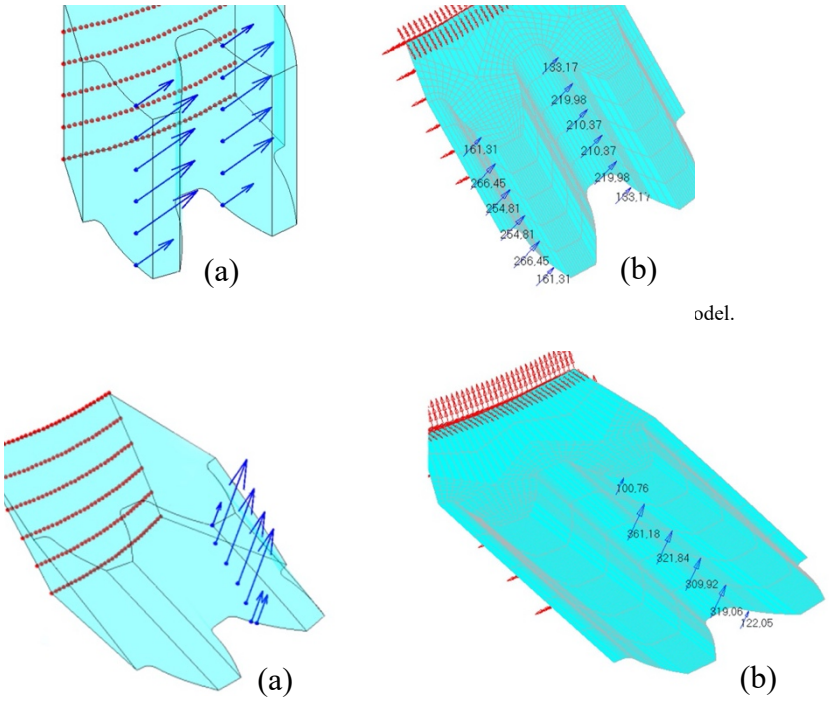

Fig. 11. Single contact in helical gear (Case 3): (a) in SA model, (b) in FE model.

The displacements related to the contact nodes results are compared with analogous FE models in Figures 12, 13 and 14: no relevant differences are appreciated, except the two first contact nodes of Case 3 with a discrepancy of 2%.

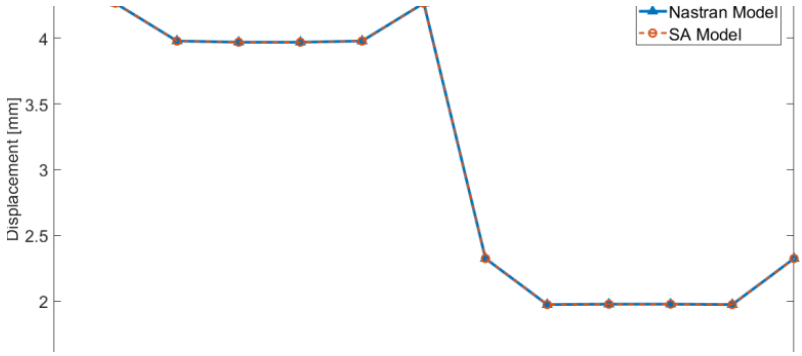

Fig. 12. Contact node displacement comparison in standard spur gears (Case 1).

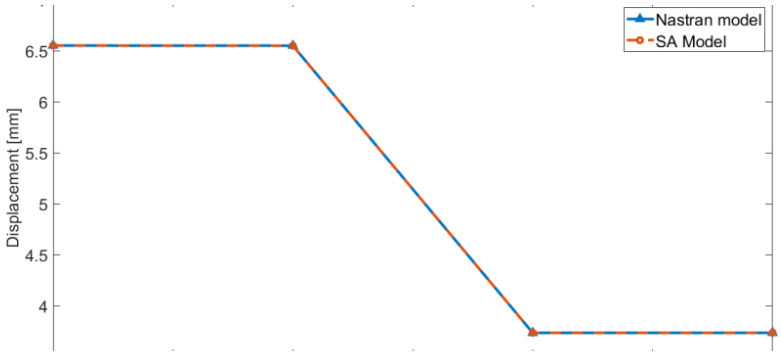

Fig. 13. Contact node displacement comparison in crowned spur gears (Case 2).

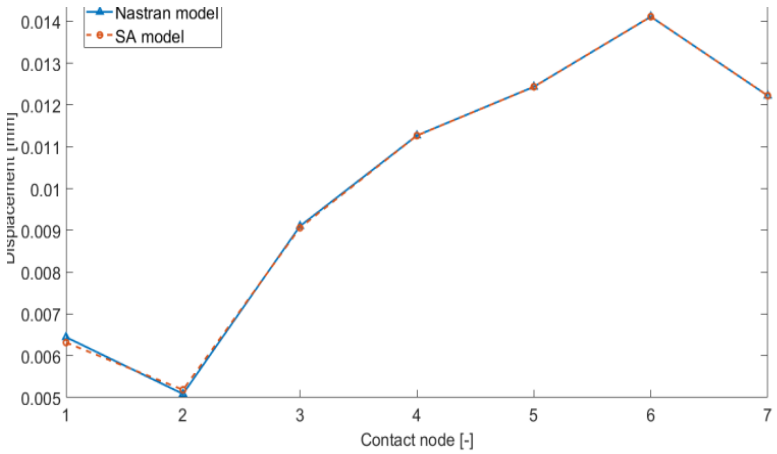

Fig. 14. Contact node displacement comparison in helical gears (Case 3).

3.2. Static transmission error: results and comparison

Applying the formulas cited in Paragraph 3.1 to the non-deformed profile of each tooth in contact is possible to evaluate the total deformation; the STE is then calculated as the angular rotation of the gear due to the deformations under the exchanged load:

$$STE = \theta_1 - \theta_2 \tag{1}$$

As far as the contact point converges in the equilibrium condition the algorithm iterates. When the contact points finally find their equilibrium position, the algorithm passes to the next angular position, as shown in Figure 2.
To highlight the changes made by the implementation of the 3D local contact model, a comparison with the previous 2D model is presented. The results refer to two standard spur gears with no surface modification, whose parameters are listed in Table 4, because of the limits imposed to the geometries by the 2D model.

Table 4. Input parameters for the geometric coordinates of the gears.

Gear parameters	Gear1 nomenclature	Gear2 nomenclature
Number of teeth [-]	28	28
Tooth module [mm]	3.175	3.175
Face-width [mm]	6.35	6.35
Hub radius [mm]	20	20
Pressure angle [°]	20	20

In Figure 15, the graphs are related to the SA 3D model and an equivalent FE model. For simplicity, the only iterative calculation has been done on the contact algorithm, therefore the central zone related to the single contact occupies a wider range of angular positions; furthermore, for the same reason the mean value of the double-contact is higher than FE model's STE.

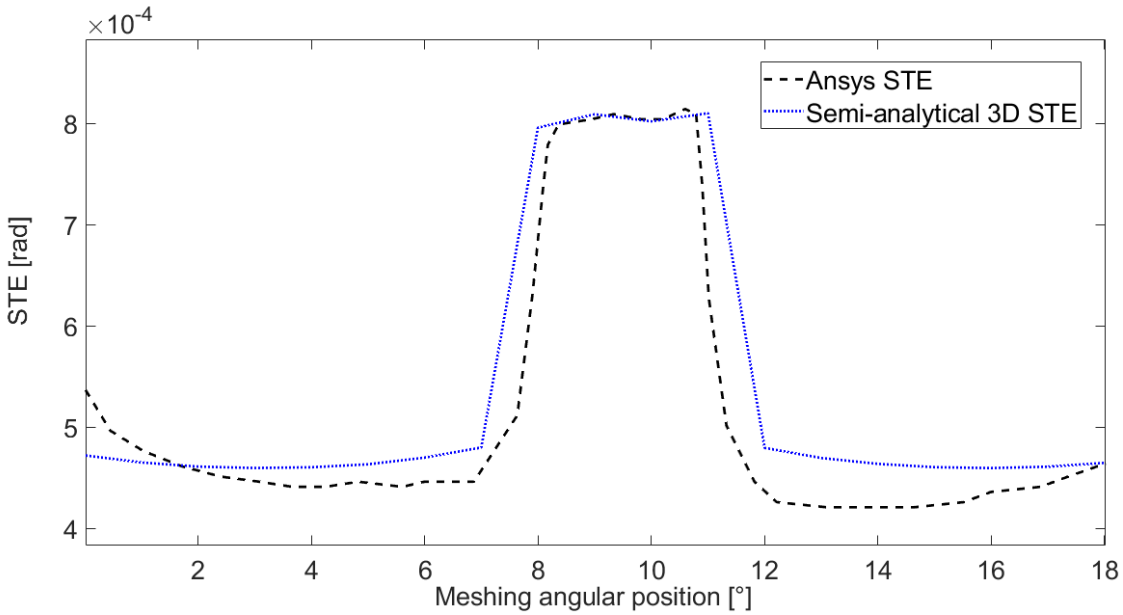

Fig. 15. STE comparison between 3D model and FE model.

4. Conclusion

In the present paper, the authors developed a semi-analytical model for the evaluation of the displacements and the static transmission error between two loaded gears of any type of geometry and with any kind of surface modifications.

Inserting a limited number of input parameters, the algorithm automatically resolves the quasi-static problem of two gears meshing, providing different output such as pressure distribution, contact area and pressure peaks. It is important to control these parameters to guarantee a transmission with a uniform use of the teeth material, avoiding peaks of pressure or flank regions that are more stressed than others. In fact, the analysis shows how the geometry of the contact area and the distribution of pressure is significantly controlled by micro-geometry modifications. Typically, edge and corner contact should be avoided not to occur in pressure peaks that can become crucial in dynamic conditions. Other output consists of the computation of the local, bending and shear, root and rim and gear body displacements: these displacements contribute to the overall deformation of the gears and therefore to the static transmission error, which is the main source of noise, vibration and harshness.

Modifying the geometry of the teeth and the gear body it is possible to control the resultant shape of the static transmission error; in general, the peak-to-peak transmission error should be reduced to excite the system less.

The proposed methodology is implemented in a code called GeDy TrAss (acronym of Gear Dynamics Transmission Analysis) that has been developed by the homonymous company GeDy TrAss s.r.l. This tool is useful in the pre-design phase of mechanical transmissions to understand which geometry would fit a certain quasi-static operative condition in the best way.

Acknowledgements

The authors would like to thank GeDy TrAss s.r.l. for granting the software for research purpose and allowing the publication of this paper.

References

Attia, A. Y., 1964. Deflection of spur gear teeth cut in thin rims. Journal of Engineering for Industry 86(4), 333–341.

Beghini, M., Santus, C., 2004. Analysis of the contact between cubic profiles. International journal of Mechanical Sciences 46, 609–621.

Boedo, S., 2013. A corrected displacement solution to linearly varying surface pressure over a triangular region on the elastic half-space. Tribology International 60, 116–118.

Cornell, R. W., 1981. Compliance and stress sensitivity of spur gear teeth. Journal of Mechanical Design 103(2), 447–459.

Johnson, K. L., 1985. Contact mechanics. Cambridge University Press, UK.

Li, J., Berger, E. J., 2003. A semi-analytical approach to three-dimensional normal contact problems with friction. Computational Mechanics 30, 310–322.

Marmo, F., Sessa, S., Rosati, L., 2016. Analytical solution of the Cerruti problem under linearly distributed horizontal pressures over polygonal domains. Journal of Elasticity 124, 27–56.

Marmo, F., Toraldo, F., Rosati, A., Rosati, L., 2018. Numerical solution of smooth and rough contact problems. Meccanica 53(6), 1415–1440.

Rosso, C., Bruzzone, F., Maggi, T., Marcellini, C., 2019. A proposal for semi-analytical model of teeth contact with application to gear dynamics. JSAE/SAE 2019. Kyoto, Japan.

Rosso, C., Bruzzone, F., Maggi, T., Marcellini, C., 2018. Method for determining the tooth deformation, preferably for the static transmission error of gears. P2912IT00.

Sainsot, P., Velex, P., Duverger, O., 2004. Contribution of gear body to tooth deflections, a new bidimensional analytical formula. Journal of Mechanical Design 126, 748–752.